Chemically Homogeneous Complex Oxide Thin Films Via Improved Substrate Metallization

*Christopher T. Shelton, Paul G. Kotula, Geoff L. Brennecka, Peter G. Lam, Kelsey E. Meyer, Jon-Paul Maria, Brady J. Gibbons, and Jon F. Ihlefeld**

A long-standing challenge to the widespread application of complex oxide thin films is the stable and robust integration of noble metal electrodes, such as platinum, which remains the optimal choice for numerous applications. By considering both work of adhesion and stability against chemical diffusion, it is demonstrated that the use of an improved adhesion layer (namely, ZnO) between the silicon substrate and platinum bottom electrode enables dramatic improvements in the properties of the overlying functional oxide films. Using $BaTiO_3$ and $Pb(Zr,Ti)O_3$ films as test cases, it is shown that the use of ZnO as the adhesion layer leads directly to increased process temperature capabilities and dramatic improvements in chemical homogeneity of the films. These result in significant property enhancements (e.g., 300% improvement to bulk-like permittivity for the $BaTiO_3$ films) of oxide films prepared on Pt/ZnO as compared to the conventional Pt/Ti and Pt/TiO_x stacks. A comparison of electrical, structural, and chemical properties that demonstrate the impact of adhesion layer chemistry on the chemical homogeneity of the overlying complex oxide is presented. Collectively, this analysis shows that in addition to the simple need for adhesion, metal-oxide layers between noble metals and silicon can have tremendous chemical impact on the terminal complex oxide layers.

1. Introduction

Enabling broad impact utilizing the tremendously varied properties available in complex oxide thin films requires a means of integration on technologically relevant substrates, specifically mainstream semiconductors such as silicon. Many such devices require substrate metallization to form electrical contacts, and the most widely and technologically relevant is platinum-coated silicon. Platinized silicon offers great flexibility in being chemically inert in contact with many oxides, compatible with moderate processing temperatures in oxidizing, inert, or moderately-reducing atmosphere (thus requiring little or no process alteration for integration with any of a variety of complex film systems), and is relatively inexpensive when used in thin layers. As such, while optimization of electrode (and/or substrate)-film interactions is emphasized for complex oxides deposited on base metals, oxide electrodes, and exotic substrates, the electrode/substrate interface is too-often simply ignored or, at best, considered entirely inert, passive observers in the integration process in the vast majority of work on platinized silicon. In spite of the extensive earlier efforts toward preparing high-quality, temperature-stable platinized silicon substrates for ferroelectric memory integration, several issues remain that are detrimental to the deposited oxide properties. The most pervasive of these are thermophysical instabilities at temperatures in excess of 700 °C including delamination and hillocking as well as diffusion of adhesion layers through the platinum; these defects often cause degraded performance and can result in inoperable devices.[1] Additionally, the (presumed) 700 °C limit for thermal processing of films on platinum-coated silicon substrates has been highlighted as the primary source of the chasm between the (poor) measured properties of refractory oxides such as $BaTiO_3$ films on silicon wafers and the bulk-like behavior that has been achieved by processing these films at higher temperatures on other substrates.[2,3] Extensive research efforts by many groups have investigated the causes of and solutions to these issues. Several reports indicate that zirconium,[1,4,5] tantalum,[5] titanium oxide,[1,4,6,7] and aluminum oxide[8] adhesion layers are superior to the more common titanium in terms of lower diffusivity through the platinum layer, limited reaction with the underlying substrate, and a lack of polymorphic phase changes over the desired processing temperature range resulting in fewer mechanical defects (delamination, roughening, and hillocking). These advances notwithstanding, titanium adhesion layers remain the most widespread.

C. T. Shelton,[+] Dr. P. G. Kotula, Dr. G. L. Brennecka, K. E. Meyer, Dr. J. F. Ihlefeld
Materials Science and Engineering Center
Sandia National Laboratories
Albuquerque, NM, 87185, USA
E-mail: jihlefe@sandia.gov

Dr. P. G. Lam, Prof. J.-P. Maria
Department of Materials Science and Engineering
North Carolina State University
Raleigh, NC, 27695, USA

Prof. B. J. Gibbons
Materials Science, School of Mechanical, Industrial, and Manufacturing Engineering
Oregon State University
Corvallis, OR, 97331, USA

[+] Present address: Department of Materials Science and Engineering, North Carolina State University, Raleigh, NC 27695, USA

DOI: 10.1002/adfm.201103077

Considerations for proper adhesion layers include chemical compatibility with the substrate and platinum, phase stability, interfacial energy, and stability against chemical diffusion. Inspection of the list of materials investigated previously indicates that many of these, in their oxide form, do not form low energy interfaces with common electrode metals. Large contact angles (≈120°) and concomitantly low work of adhesion values (<1 J m^{-2}) are observed for relatively noble metals copper, silver, and nickel on ZrO_2;[9] similarly high contact angles of 124° are observed for gold on TiO_2;[10] and while alumina adhesion layers have shown reasonable stability to high temperatures,[8] metals such as gold and copper have large contact angles (≈130° and ≈125°, respectively)[10,11] and low work of adhesion values (≈0.6 J m^{-2} for copper/Al_2O_3) and a similarly low work of adhesion for platinum 1.05 J m^{-2} has been reported.[12] Contrasting these values with those observed for copper, which is isostructural with platinum, wetting ZnO reveals a low contact angle of 62° and a high work of adhesion of 2.01 J m^{-2} that is twice as large as any reported for other investigated adhesion layers.[11] This high work of adhesion suggests that ZnO may be an excellent adhesion layer for metal electrodes by providing a low energy interface between the metal film and buffer oxide. While none of the traditional adhesion layer metals are thermodynamically stable in contact with platinum for conventional processing temperatures (phase diagrams reveal a number of intermetallic phases for each), the adhesion layer oxides are, in general, thermodynamically stable. Most common metallic adhesion layers (Zr and Ta) oxidize quickly during processing and remain relatively stable (albeit with poor adhesion).[5] There is, however, a precedent for titanium to readily diffuse through the platinum electrode and form a thin layer on the platinum surface.[4,5,7,13] In this report it is shown that ZnO-buffered platinum films maintain mechanical integrity to higher temperatures than typical titanium and titanium oxide buffered substrates owing to improved wetting. Further, it is demonstrated that these substrates can be used to dramatically improve the performance of two prototypical complex oxide thin films by 1) allowing access to previously difficult to realize processing temperatures and 2) minimizing chemical heterogeneities directly related to diffusion of buffer layer species through the electrode.

2. Results and Discussion

To test the applicability of ZnO as an adhesion layer for platinized silicon substrates, we have prepared a series of platinum films on silicon substrates with traditional titanium, titanium oxide, and zinc oxide buffers via radio frequency (RF)-magnetron sputtering. The general structure is as follows: 100 nm platinum/40 nm buffer/400 nm SiO_2/(001)-oriented silicon. Titanium and titanium oxide films were prepared by sputtering from a titanium target. Titanium oxide was formed by heating the titanium coated substrate in vacuo to 400 °C in 15 mTorr of oxygen for 30 min;[1] as the precise phase and oxidation state is unknown, we will denote the titanium oxide buffer as TiO_x throughout this text. Zinc oxide buffer layers were deposited from a sintered ceramic target. All buffer layers were capped with platinum without breaking vacuum. In each case predominantly (111)-oriented platinum was observed via X-ray diffraction. For the ZnO-buffered film, only the peak attributed to the 0002 reflection of ZnO could be observed, indicating that the ZnO is deposited with a preferential *c*-axis orientation.

To investigate the thermal stability, platinum films were processed ex situ in air by annealing at temperatures ranging from 500 °C to 900 °C for 1 h. **Figure 1** shows representative scanning electron microscopy (SEM) images for the platinum films annealed at 700, 800, and 900 °C with the three different buffer layers. Distinct differences in the platinum microstructure with adhesion layer and annealing temperature can be observed. For films processed on titanium buffer layers, a microstructure showing voids in the platinum layer is evident at 800 °C with significant dewetting occurring by 900 °C. Films on TiO_x buffer layers appear to be more robust and exhibit dewetting behavior at 900 °C. Small dark areas at the platinum grain boundaries are observed in the SEM images for the films on titanium and TiO_x buffer layers. This is consistent with electron emission from a lower atomic number material and is indicative of the presence of titanium on the surface as has been observed by previous researchers.[13] For each processing condition, films on ZnO buffer layers display very few voids in the platinum layer and possess larger platinum grains. This data is consistent with platinum preferentially wetting the ZnO adhesion layer.

To assess the performance of the ZnO-buffered platinized silicon substrates for complex oxide thin film applications, we prepared traditional ferroelectric thin films, $PbZr_{0.52}Ti_{0.48}O_3$ (PZT) and $BaTiO_3$, via chemical solution deposition (CSD) on each of the titanium-, TiO_x-, and ZnO-buffered substrates. PZT films were processed at 700 °C, as is conventional for device quality material,[14] and $BaTiO_3$ films were processed at 900 °C, a condition that is traditionally unattainable on platinized silicon substrates and that has previously been shown to enable bulk-like dielectric responses.[2,3,15]

X-ray diffraction (Supporting Information, Figure S1) data for the PZT films reveals phase-pure material with peaks only attributable to the film and substrate layers. The films possess no preferred crystallographic orientation, as the peak intensity ratios are consistent with a powder sample. The lack of texture likely stems from the rapid heating rate used during crystallization.[16] **Figure 2** shows plan-view and cross-sectional SEM images of the PZT films on each substrate. The films are composed of a dense columnar microstructure with slight differences in the average grain lateral dimensions spanning 87 ± 27 nm, 80 ± 9 nm, and 109 ± 9 nm for Ti-, TiO_x-, and ZnO-buffered films, respectively. Evidence of a surface fluorite secondary phase is observed on the Ti-buffered films for these processing conditions and result in increased error in grain size measurements. The cause of this is unclear, however we note that it appears to be present as a very thin discontinuous layer on the film surface and is generally associated with lead deficiency.[17–19] In cross-section, the differences in the substrate metallization can be appreciated. The titanium layer in the Ti-buffered film shows evidence of roughening, likely due to oxidation and grain growth, whereas the TiO_x- and ZnO-buffer layers remain relatively smooth. This is consistent with relatively smooth platinum films at these temperatures as investigated in the ex situ annealing study.

Polarization-electric field measurements were performed to assess the ferroelectric properties of the PZT films on the

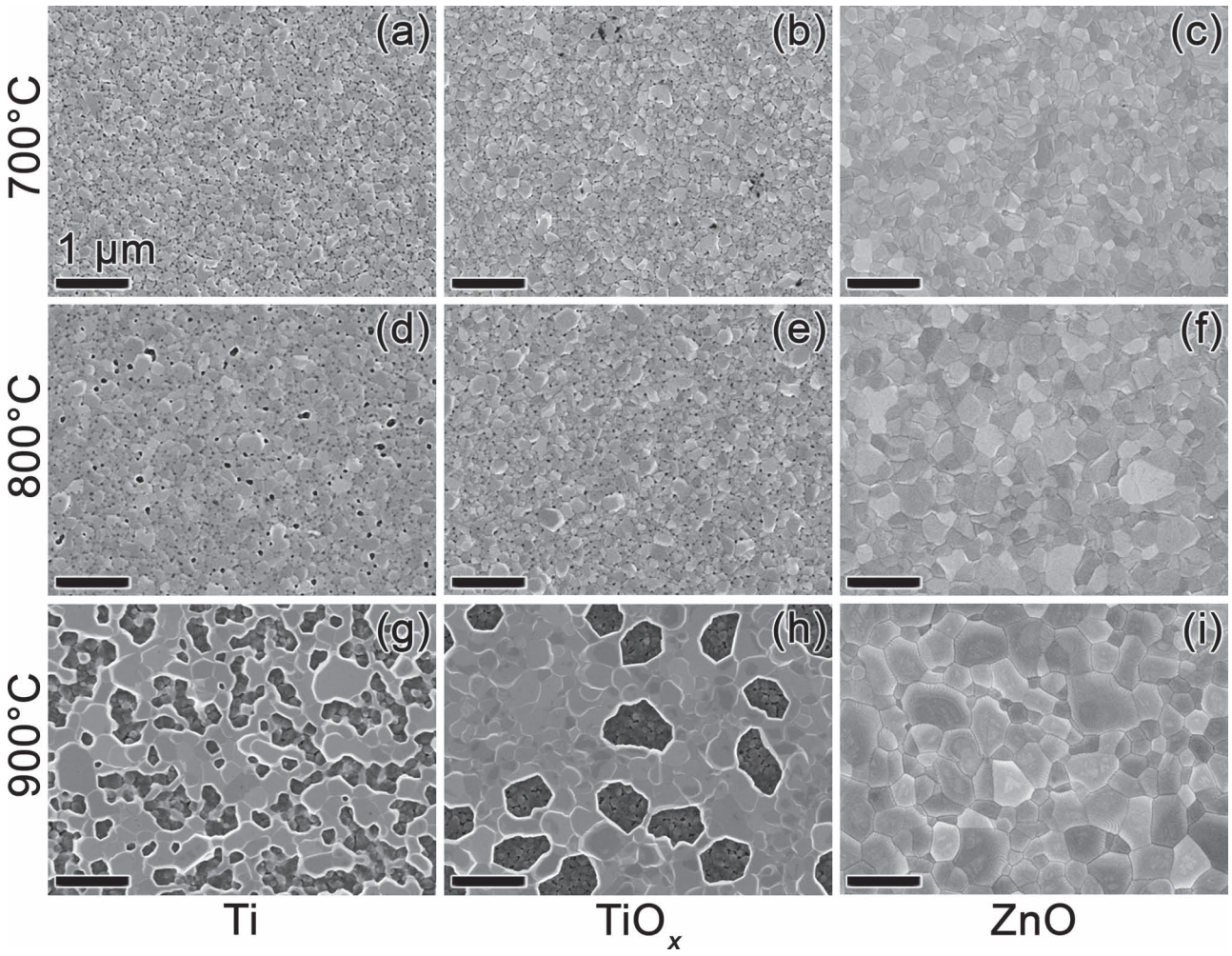

Figure 1. Plan-view SEM images of platinum films deposited titanium-buffered (a,d,g), titanium oxide buffered (b,e,h), and zinc oxide buffered (c,f,i) SiO_2/silicon substrates and annealed for 1 h in air at 700 °C, 800 °C, and 900 °C.

different substrates. Nested hysteresis loops were measured at 10 Hz for each film, with the results shown in **Figure 3**. In each case well saturating loops are observed, suggesting minimal contributions from electrical leakage. Remanent polarization and coercive field values for films on each substrate are noted on the figures. In comparing these values, a performance improvement on the ZnO-buffered substrates becomes evident; a remanent polarization increase of nearly 35% from 23 μC cm^{-2} to 32 μC cm^{-2} is observed between the traditional Ti- and new ZnO-buffered films. This increase in remanent polarization is accompanied by a decrease in coercive field from 47 kV cm^{-1} to 43.8 kV cm^{-1}. In addition to enhanced ferroelectric response, dielectric properties also are enhanced. Supporting Information Figure S2 shows permittivity versus applied electric field measurements for each film. Nearly identical high-field response is observed with permittivities saturating to approximately 260 at 500 kV cm^{-1} and loss tangents of 0.015 (1.5%). At low fields, increases in the magnitude of the responses are observed as the zero bias

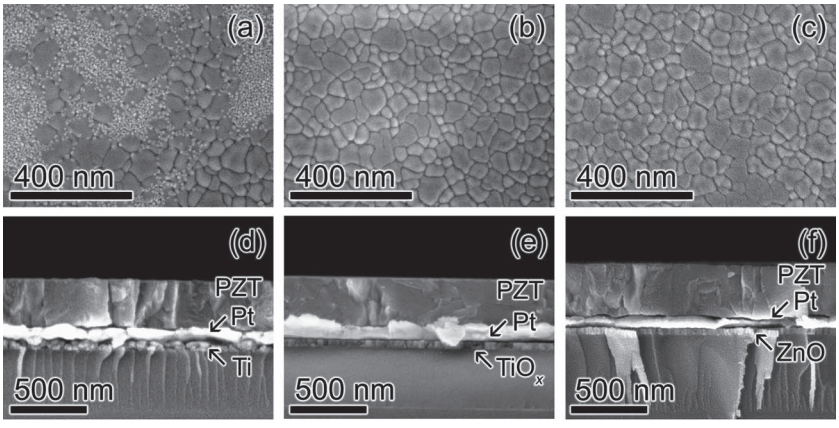

Figure 2. Plan-view and cross-sectional SEM images of $Pb(Zr,Ti)O_3$ thin films deposited on ZnO-buffered (a,d), TiO_x-buffered (b,e), and titanium-buffered (c,f) platinized silicon substrates.

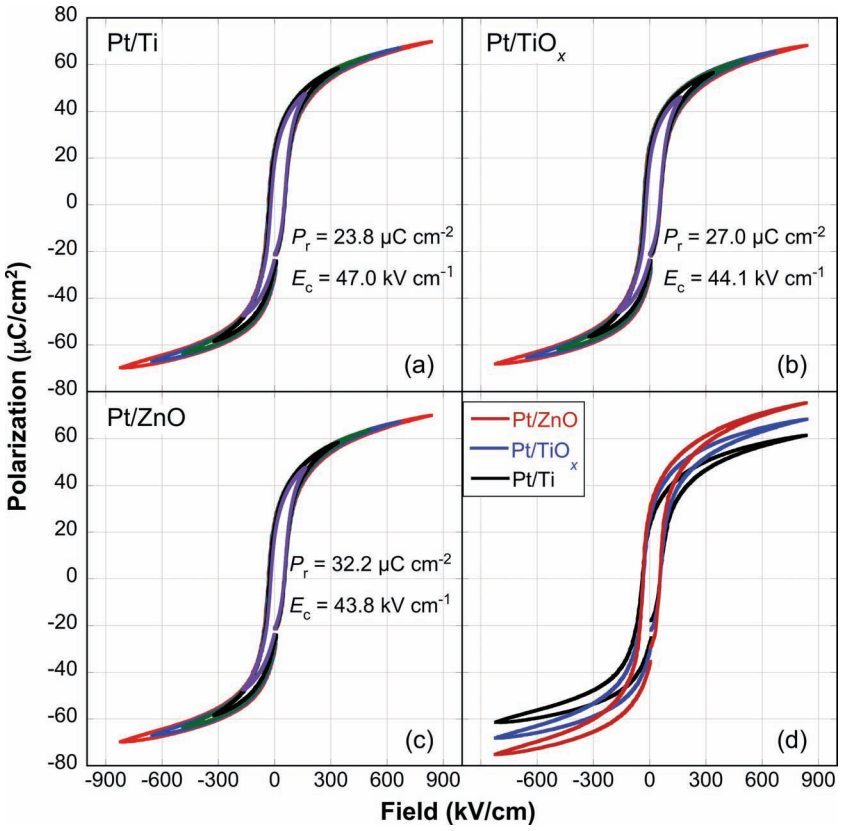

Figure 3. Polarization versus electric field loops collected at 10 Hz for Pb(Zr,Ti)O_3 films deposited on a) titanium-buffered, b) TiO_x-buffered, and c) ZnO-buffered platinized silicon substrates. d) A comparison of the films on each substrate.

and peak permittivities increase when the buffer changes from titanium to TiO_x and ZnO, respectively, with the film on ZnO-buffered platinum having a zero bias value of ca. 1600 and peak value approaching 2000 at the coercive field. Enhancements in both dielectric constant and polarization coupled with the random crystallographic orientations of all films in the study demonstrate that a simple crystallographic texturing argument cannot explain the improvements afforded through use of the ZnO-buffered substrate.

From the substrate annealing study, mechanical integrity of the ZnO-buffered films persisted to higher temperatures, as would be expected for an interface with a high work of adhesion. To assess the high-temperature applicability of these substrates, $BaTiO_3$ films were prepared and processed to 900 °C. X-ray diffraction patterns for each film are shown in Supporting Information Figure S3; in each case phase-pure randomly oriented material is observed. Plan-view and cross-sectional SEM images for $BaTiO_3$ films on each substrate are shown in **Figure 4**. Similar ceramic film microstructures are observed for each film. Average grain diameters for the $BaTiO_3$ films are 44 ± 4 nm, 62 ± 6 nm, and 55 ± 11 nm for Ti-, TiO_x-, and ZnO-buffered films, respectively. As was observed for the PZT films, microstructural differences are identified in the electrode stacks in cross section. Both the Ti- and TiO_x-buffered platinum layers appear rough and possess voids. The platinum film on ZnO, however, remains relatively smooth, consistent with the platinum annealing study and a low wetting angle. The cross-sectional microstructure of the $BaTiO_3$ films reveals finite porosity levels that are uniformly distributed throughout the thickness for each film. Some thickness differences are observed with average film values of 215, 202, and 178 nm for films on Ti-, TiO_x-, and ZnO-buffered substrates, respectively, indicating possible improved density for films on TiO_x- and ZnO-buffered substrates. Some fine cracks are visible in the plan-view image and are likely due to the high coefficient of thermal expansion mismatch between $BaTiO_3$ and silicon.[20]

Fine cracks, such as those seen in these $BaTiO_3$ films, preclude high-field measurements. However, temperature dependence of the dielectric response is a broadly accepted means to characterize $BaTiO_3$-based materials. The dielectric properties were compared for the $BaTiO_3$ films by performing temperature dependent permittivity and dielectric loss measurements between 180 and 500 K (at 1 kHz) as shown in **Figure 5**. For each film the loss values remain less than 5% (tan $\delta < 0.05$) over the entire measurement range. Relatively flat permittivity responses are observed, consistent with the fine grain size,[21] however, a striking difference in the magnitude of the relative permittivity was observed; the films deposited on the titanium- and TiO_x-buffered substrates had peak permittivities of less than 350 while the film deposited on the ZnO-buffered substrate possessed a peak permittivity of 1380, representing a nearly 300% increase.

Unambiguous improvements in the ferroelectric and dielectric responses were observed for both PZT and $BaTiO_3$ films

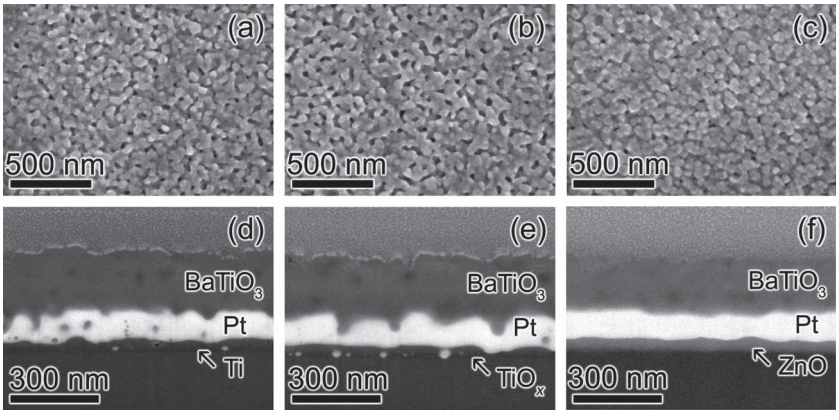

Figure 4. Plan-view and cross-sectional SEM images of $BaTiO_3$ thin films deposited on ZnO-buffered (a,d), TiO_x-buffered (b,e), and titanium-buffered (c,f) platinized silicon substrates. Cross-sections were prepared via focused Ga^+ ion beam milling.

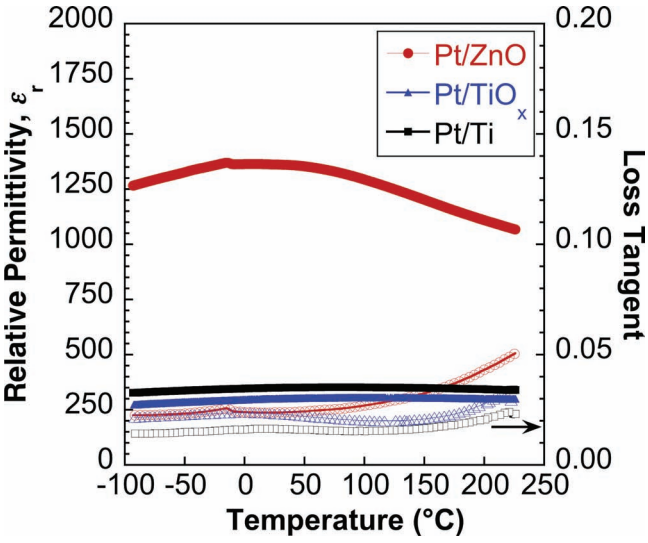

Figure 5. Temperature dependence of permittivity (solid markers) and loss tangent (open markers) for barium titanate thin films deposited on titanium-, TiO_x-, and ZnO-buffered platinized silicon substrates.

deposited on ZnO-buffered substrates. The properties measured for PZT films appear to be the best reported to date. Likewise, the permittivity approaching 1400 for the $BaTiO_3$ film of grain size 55 nm falls on the grain size-permittivity master curve that normally is reserved for well-prepared fine-grained bulk ceramics[21] and thin films processed on base-metal or refractory substrates[2] and represents among the highest recorded values for a $BaTiO_3$-based film deposited on a silicon substrate[8,22,23] and possibly the highest devoid of a columnar grain morphology. This high permittivity is even more striking when considering the relatively low thickness of the film and the known thickness scaling effects in ferroelectric thin films.[24] Given that the microstructural differences for films on each substrate are relatively minor (similar grain dimensions and porosity levels) some other attribute(s) must be responsible.

To elucidate the differences resulting in the improved ferroelectric and dielectric performance on ZnO-buffered substrates, quantitative chemical mapping using multivariate statistical analysis (MSA) with energy dispersive spectroscopy in a scanning transmission electron microscope (STEM-EDS) for the PZT and $BaTiO_3$ films was conducted, as described previously.[25] **Figure 6** shows titanium composition maps and integrated distribution profiles for profiles for lead, zirconium, and titanium for the three PZT films on the different substrates. Supporting Information Figure S4 shows the STEM-EDS composition maps for lead and zirconium for each film. Distinct differences in the cation distributions are observed. The films processed on the titanium- and TiO_x-buffered substrates possess enriched concentrations of titanium near the platinum/PZT interface, while the film surfaces are enriched in both zirconium and lead. This inhomogeneous cation distribution has been observed by several groups depositing PZT via chemical solution routes and has been generally ascribed to the lower

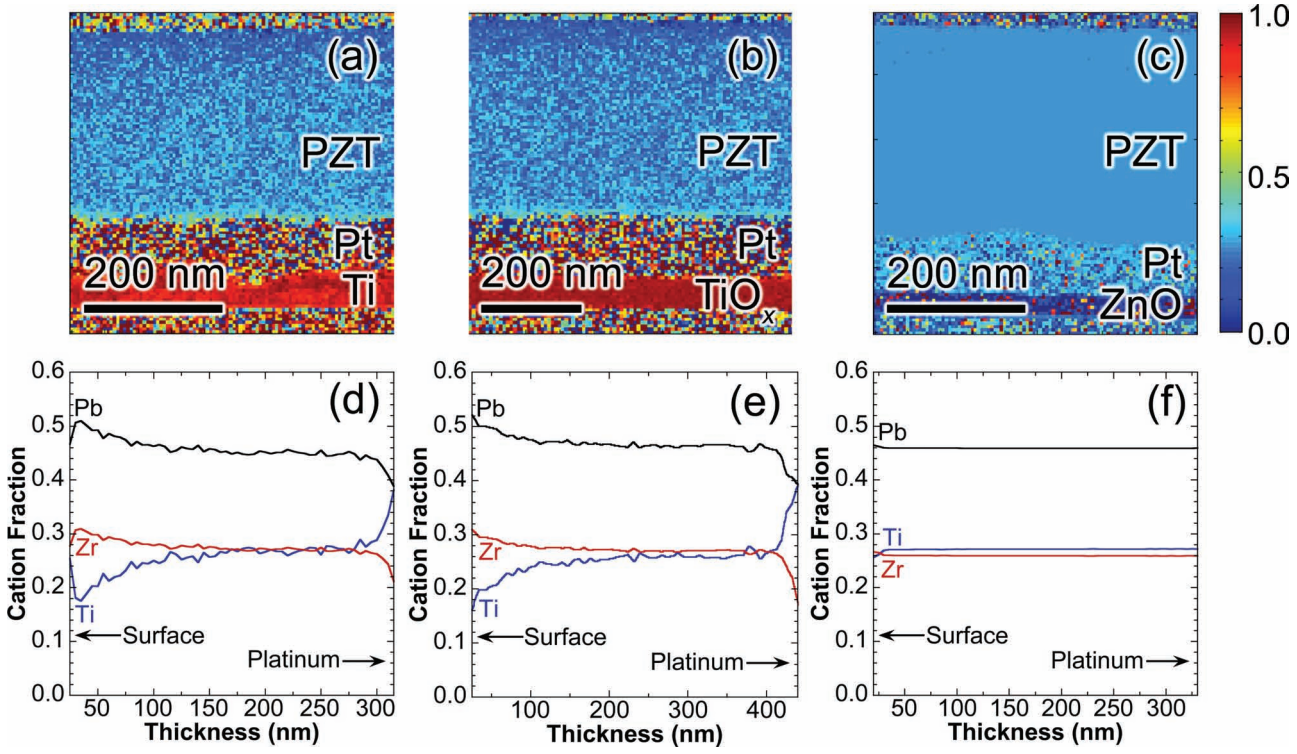

Figure 6. Quantified composition maps of titanium ions and quantified lead, zirconium and titanium cation distributions through the thickness of $Pb(Zr,Ti)O_3$ films deposited on titanium-buffered (a,d), TiO_x-buffered (b,e), and ZnO-buffered (c,f) platinized silicon substrates. Note that the quantification algorithm in regions that nominally do not contain titanium (e.g., platinum electrodes) results in amplification of measurement noise and is not representative of actual titanium concentrations.

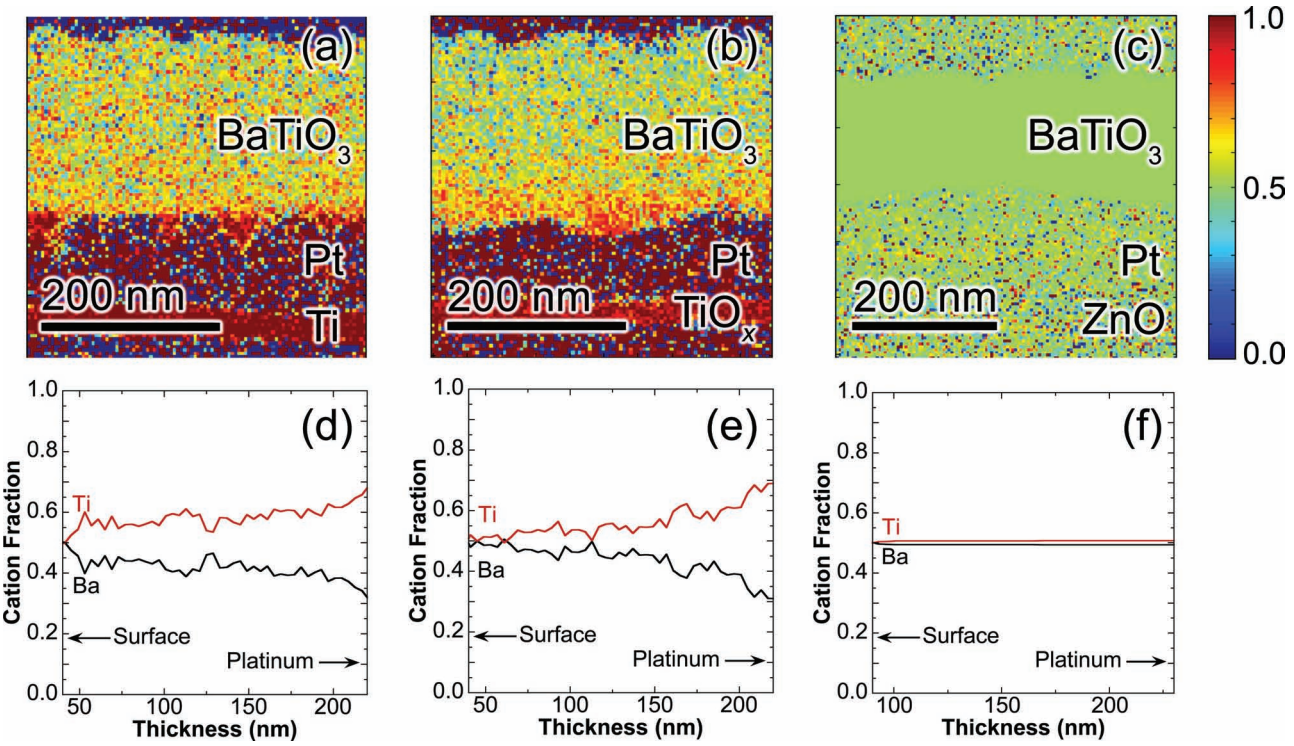

Figure 7. Quantified composition maps of titanium ions and quantified barium and titanium cation distributions through the thickness of $BaTiO_3$ films deposited on titanium-buffered (a,d), TiO_x-buffered (b,e), and ZnO-buffered (c,f) platinized silicon substrates.

nucleation barrier for $PbTiO_3$ on the platinum surface versus $PbZrO_3$.[26–29] The film deposited on the ZnO-buffered platinum substrate shows virtually no composition gradient through the film thickness. In addition to the improved zirconium and titanium distributions, lead also remains evenly distributed with no surface enrichment.

Figure 7 shows the titanium composition maps and integrated distribution profiles for barium and titanium in the $BaTiO_3$ films. Composition maps for barium can be found in Supporting Information Figure S5. Similar to that observed in the PZT films, we see clear composition gradients in films processed on titanium and titanium oxide buffered substrates. Titanium enrichments of greater than 10% are observed near the platinum interface and the stoichiometry approaches unity near the film surfaces. $BaTiO_3$ films processed on ZnO-buffered substrates, however, possess minimal heterogeneities in cation distribution with both the barium and titanium concentrations remaining nearly flat throughout the thickness (a narrow compositional scale map and integrated profile for the $BaTiO_3$ film on ZnO can be found in Supporting Information Figure S6). It is interesting to note that no secondary phases were observed in the X-ray diffraction patterns or in TEM even with the substantial non-stoichiometry near the platinum interface. This is consistent with the limited thermal budget used in the thin film processing, which allows for broader single-phase fields.[30]

The improvements in chemical homogeneity for films on ZnO-buffered substrates correspond directly with the enhancements in dielectric and ferroelectric properties. For the PZT films we observe the highest remanent polarization and permittivity and lowest coercive fields for films devoid of chemical gradients. In bulk ceramic materials peaks in remanent polarization and permittivity and a minimum in the coercive field are observed near the morphotropic phase boundary (MPB); compositions deviating by as much as 15% percent from the MPB, particularly toward titanium-rich compositions, possess decreased polarization and permittivity and increased coercivity.[31,32] The chemically homogeneous film has a composition very near this boundary while chemically heterogeneous films have compositions that deviate by several percent from this composition spatially throughout the film thickness. The diminishing properties scale similarly with those expected for non-MPB compositions and this appears to be the primary cause of the observed trends. Likewise, the dramatic improvements in $BaTiO_3$ permittivity appear to be directly related to the improved chemical homogeneity. We have previously observed that titanium-rich $BaTiO_3$ films processed to identical temperatures tend to possess severely diminished dielectric constants.[33] This same phenomenon appears to be responsible for the limited dielectric permittivity in the films possessing a chemical gradient–and apparent titanium enrichment.

We contend that titanium from the titanium and TiO_x buffer layers diffuses through the platinum electrode and reacts with the PZT and $BaTiO_3$ film precursors causing chemical heterogeneities that result in diminished ferroelectric and dielectric responses. While diffusion of titanium through the platinum film when using a titanium adhesion layer may be expected based upon previous work,[4,7,13,34,35] it is somewhat surprising that such an action would be observed from the TiO_x adhesion layers.[4,7] We speculate that the TiO_x layer is oxygen deficient and titanium is diffusing through the platinum in order to

reach a lower free energy oxide state. The presence of a fluorite phase on the surface of the PZT film on titanium-buffered platinum is consistent with this model. Excess titanium diffusing from the adhesion layer would consume excess lead in the film, effectively acting as lead sink. This would result in net lead deficiency in the film, which commonly manifests as a finite amount of fluorite phase on the film surface. With the substitution of ZnO for titanium in the electrode stack, not only is the integrity of the platinum electrode improved in both continuity and elimination of voids owing to improved wetting, but additionally its chemical stability eliminates an extrinsic source of cations from diffusing into the overlaying film and allows for the fabrication of high-quality, chemically homogeneous complex oxide thin films.

It is important to comment that previous work on solution-deposited PZT has shown chemical gradients in films with multiple deposition and firing steps, resulting in a 'saw-tooth' composition profile.[29,36] Because these prior reports observed chemical gradients even in layers deposited directly on previously crystallized PZT layers and might therefore be expected to be free from chemical influence of the buffer layer, this result would seem at odds with our observations that appear to directly link the presence of a chemical gradient with chemical influence from the buffer layer. At this time the specific mechanisms at play are not fully understood, but we note that the solution chemistry used in this work is different than the traditional methoxyethanol-based sol-gel chemistry used by other groups and this may have an influence on the crystallization behavior.

3. Conclusions

In summary, this work demonstrates that dramatic improvements in metallization integrity and electroceramic thin film performance can be appreciated by properly selecting materials to minimize interfacial energy between metallization and adhesion layers. Opportunities to utilize this same metallization/buffer layer embodiment likely exist for a broad range of applications beyond ferroelectric capacitors, including microelectromechanical systems, microprinted heaters and sensors, and electrochemical energy storage, where integrity of metallized silicon to high temperatures is necessary. We have demonstrated improved ferroelectric and dielectric response in two ferroelectric thin film materials, PZT and $BaTiO_3$, and have correlated this enhanced performance, including the best known properties ever reported for each of these materials on silicon, to greatly improved chemical homogeneity, which is a direct result of deposition on ZnO-buffered substrates. We believe that this work has broad implications for electroceramic thin film synthesis. First, we have identified a substrate metallization scheme utilizing an adhesion layer that has a high work of adhesion, which in turn enables processing under thermal budgets typically reserved for more exotic ceramic, single-crystal, or metal foil substrates. Second, this data provides evidence that the commonly observed titanium enrichment at the PZT/Pt interface is amplified by a thin titanium-containing layer on the platinum surface that diffuses from the buffer layer. By eliminating titanium from the metallization process there is no longer an extrinsic titanium source to drive lead titanate nucleation and the resulting composition gradient. Third, $BaTiO_3$ films with bulk-like dielectric properties have been prepared on a silicon substrate. This demonstration presents a means of overcoming the historical barrier to preparing high-quality complex oxide films on conventional silicon substrates. Finally, by eliminating the extrinsic source of titanium, materials of higher purity and chemical uniformity can be prepared and will allow researchers to study intrinsic material properties where data is not obscured by unintentional contamination.

4. Experimental Section

Commercial 75 mm silicon wafers with 4000 Å of thermal oxide (Silicon Quest International Inc.) were used as starting substrates. All metal and buffer layer films were deposited via RF magnetron sputtering from 4 in. targets. 40 nm thick titanium was deposited at room temperature from a titanium target with a power density of 6.6 W cm^{-2} and an argon background pressure of 3 mTorr. Titanium oxide (TiO_x) was prepared identically and the chamber background pressure was altered to 15 mTorr O_2 and the substrate heated to 400 °C for 30 min prior to cooling to room temperature. Zinc oxide was deposited from a sintered ZnO target with a power density of 1.85 W cm^{-2} in a chamber background pressure 5 mTorr composed of a 2:1 ratio of Ar:O_2. Platinum films were deposited from a platinum target with a power density of 6.6 W cm^{-2} and argon background pressure 3 mTorr. All films were deposited in vacuo. The platinum annealing study was performed by dicing the wafers and annealing in air at temperatures ranging from 500 °C to 900 °C for 1 h with direct insertion into a tube furnace at the annealing temperature.

$PbZr_{0.52}Ti_{0.48}O_3$ solutions were prepared via an inverted-mixing order chelate chemistry originally described elsewhere.[37] Titanium isopropoxide and zirconium butoxide (80% in butanol) were combined and chelated with 4 molar equivalents of acetic acid. Methanol was added and the solution heated to 90 °C and 20 mole percent excess lead (IV) acetate was added and dissolved. The solution was then cooled to room temperature and diluted with sequential additions of methanol and acetic acid resulting in a 0.35 M solution. Films were deposited via spin casting at 4000 rpm for 30 s and then placed on a 350 °C hotplate for 1 min and the process repeated three times. The films were then annealed at 700 °C in air in a preheated furnace for 10 min for crystallization. $BaTiO_3$ solutions were prepared via a chelate chemistry chemical solution technique based on previous studies.[22,38] Titanium isopropoxide was chelated with 2 molar equivalents of 2,4 pentanedione at room temperature. Separately, a molar excess of barium acetate was dissolved in propionic acid at a concentration of 0.25 M. The barium precursor solution was then added to the titanium precursor in an amount necessary for a stoichiometric 1:1 barium:titanium ratio. The solution was then diluted to 0.15 M with methanol. Films were deposited via spin casting at 3000 rpm for 30 s and subsequently placed on a 250 °C hotplate for 5 min for solvent evaporation and gel consolidation. This spin and hotplate anneal process was repeated twice and then the films were fired in air to 900 °C for 30 min with 20 °C per min ramp rates. Film thickness was increased by repeating this process two times for a total of 9 spin cast layers. For both PZT and $BaTiO_3$ films, platinum top electrodes 100 nm thick and ≈1 mm^2 were deposited via RF magnetron sputtering through a shadow mask. Electrode areas were verified by optical microscopy and image analysis.

Grain sizes of the PZT and $BaTiO_3$ films were determined from the plan-view SEM images using a linear intercept measurement. Total line lengths of 10 to 15 μm, corresponding to greater than 130 and 250 line intersections for the PZT and $BaTiO_3$ films, respectively, were used to provide measurement statistics. Measurement error bars represent one standard deviation from the average value.

Polarization-electric field hysteresis loops were measured at 10 Hz with a Radiant Precision Workstation instrument. Dielectric properties

for both films were measured with either an Agilent 4284 or HP 4192A impedance analyzer at 1 kHz using 100 mV oscillators. Temperature-dependent measurements were performed using a modified MMR cryogenic temperature stage between 180 and 500 K with a cooling rate of 5 K min^{-1}.

Scanning electron microscopy (SEM) images were collected within a Zeiss Supra 55VP instrument. Secondary electron imaging with in-lens detector was used. A dual beam focused ion-beam (FIB) (FEI Helios NanoLab 600) instrument was used to prepare and image cross sections of the $BaTiO_3$ films. X-ray diffraction patterns were collected using a Philips MRD instrument with copper Kα radiation in standard Bragg-Brentano geometry. TEM samples were prepared via focused Ga^+ ion beam milling. Imaging was performed within a FEI Tecnai F30-ST instrument operating at 300 kV and equipped with an EDAX R-TEM energy-dispersive X-ray spectrometer. The spectral images were acquired with a 2 nm diameter spot size with a 1.5 nA current stepped at ≈4 nm intervals with 100 ms dwell per pixel. Quantitative analysis was achieved using previously determined standards for lead, zirconium, and titanium for PZT compositions[25] and a $BaTiO_3$ single crystal for barium and titanium sensitivity factors.

Supporting Information

Supporting Information is available from the Wiley Online Library or from the author.

Acknowledgements

The authors wish to acknowledge the technical assistance of Bonnie B. McKenzie, Michael J. Rye, and Dr. Nancy Missert and the research of Dr. Brian J. Laughlin, which inspired this work. Critical review of this manuscript by Dr. Bruce A. Tuttle is greatly appreciated. This work was supported by the Laboratory Directed Research and Development (LDRD) program and the National Institute of Nano Engineering (NINE) at Sandia National Laboratories. Sandia is a multiprogram laboratory operated by Sandia Corporation, a wholly owned subsidiary of Lockheed Martin Company, for the United States Department of Energy's National Nuclear Security Administration under contract DE-AC04-94AL85000.

Received: December 19, 2011
Published online: March 6, 2012

[1] H. N. Al-Shareef, D. Dimos, B. A. Tuttle, M. V. Raymond, *J. Mater. Res.* **1997**, *12*, 347.
[2] S. M. Aygun, J. F. Ihlefeld, W. J. Borland, J. P. Maria, *J. Appl. Phys.* **2011**, *109*, 034108.
[3] J. F. Ihlefeld, A. M. Vodnick, S. P. Baker, W. J. Borland, J.-P. Maria, *J. Appl. Phys.* **2008**, *103*, 074112.
[4] S. H. Kim, D. J. Kim, J. P. Maria, A. I. Kingon, S. K. Streiffer, J. Im, O. Auciello, A. R. Krauss, *Appl. Phys. Lett.* **2000**, *76*, 496.
[5] T. Maeder, L. Sagalowicz, P. Muralt, *Jpn. J. Appl. Phys. 1* **1998**, *37*, 2007.
[6] G. R. Fox, K. Suu, US *Patent* 6,682,772 **2004**.
[7] K. Sreenivas, I. Reaney, T. Maeder, N. Setter, C. Jagadish, R. G. Elliman, *J. Appl. Phys.* **1994**, *75*, 232.
[8] S. Halder, T. Schneller, R. Waser, *Appl. Phys. A-Mater. Sci. Process.* **2007**, *87*, 705.
[9] D. Sotiropoulou, P. Nikolopoulos, *J. Mater. Sci.* **1993**, *28*, 356.
[10] D. Chatain, F. Chabert, V. Ghetta, J. Fouletier, *J. Am. Ceram. Soc.* **1993**, *76*, 1568.
[11] B. J. Laughlin, PhD thesis, *Sputtered* $(Ba_x, Sr_{1-x})TiO_3$, *BST, Thin Films on Flexible Copper Foils for Use as a Non-Linear Dielectric*, North Carolina State University, Raleigh, NC, USA **2006**
[12] M. McLean, E. D. Hondros, *J. Mater. Sci.* **1971**, *6*, 19.
[13] G. R. Fox, S. Trolier-Mckinstry, S. B. Krupanidhi, L. M. Casas, *J. Mater. Res.* **1995**, *10*, 1508.
[14] G. L. Brennecka, J. F. Ihlefeld, J.-P. Maria, B. A. Tuttle, P. G. Clem, *J. Am. Ceram. Soc.* **2010**, *93*, 3935.
[15] J. Ihlefeld, B. Laughlin, A. Hunt-Lowery, W. Borland, A. Kingon, J.-P. Maria, *J. Electroceram.* **2005**, *14*, 95.
[16] K. Nittala, G. L. Brennecka, D. S. Robinson, J. L. Jones, *Adv. X-ray Anal.* **2011**, *54*.
[17] B. A. Tuttle, T. J. Headley, B. C. Bunker, R. W. Schwartz, T. J. Zender, C. L. Hernandez, D. C. Goodnow, R. J. Tissot, J. Michael, A. H. Carim, *J. Mater. Res.* **1992**, *7*, 1876.
[18] I. M. Reaney, K. Brooks, R. Klissurska, C. Pawlaczyk, N. Setter, *J. Am. Ceram. Soc.* **1994**, *77*, 1209.
[19] G. L. Brennecka, C. M. Parish, B. A. Tuttle, L. N. Brewer, M. A. Rodriguez, *Adv. Mater.* **2008**, *20*, 1407.
[20] T. Lipinsky, J. Schubert, C. Buchal, *J. Opt. Soc. Am. B-Opt. Phys.* **2005**, *22*, 913.
[21] M. H. Frey, Z. Xu, P. Han, D. A. Payne, *Ferroelectrics* **1998**, *206*, 337.
[22] S. Hoffmann, R. Waser, *J. Eur. Ceram. Soc.* **1999**, *19*, 1339.
[23] J. Sigman, G. L. Brennecka, P. G. Clem, B. A. Tuttle, *J. Am. Ceram. Soc.* **2008**, *91*, 1851.
[24] C. B. Parker, J. P. Maria, A. I. Kingon, *Appl. Phys. Lett.* **2002**, *81*, 340.
[25] C. M. Parish, G. L. Brennecka, B. A. Tuttle, L. N. Brewer, *J. Am. Ceram. Soc.* **2008**, *91*, 3690.
[26] A. Etin, G. E. Shter, S. Baltianski, G. S. Grader, G. M. Reisner, *J. Am. Ceram. Soc.* **2006**, *89*, 2387.
[27] A. Dutschke, J. Meinhardt, D. Sporn, *J. Eur. Ceram. Soc.* **2004**, *24*, 1579.
[28] K. Amanuma, T. Hase, Y. Miyasaka, *Appl. Phys. Lett.* **1994**, *65*, 3140.
[29] F. Calame, P. Muralt, *Appl. Phys. Lett.* **2007**, *90*, 062907.
[30] J. F. Ihlefeld, P. R. Daniels, S. M. Aygun, W. J. Borland, J. P. Maria, *J. Mater. Res.* **2010**, *25*, 1064.
[31] K. Carl, K. H. Härdtl, *Ber. Dtsch. Keram. Ges.* **1970**, *47*, 687.
[32] K. Carl, K. H. Härdtl, *Phys. Status Solidi A-Appl. Res.* **1971**, *8*, 87.
[33] J. F. Ihlefeld, J. P. Maria, unpublished.
[34] O. Auciello, A. R. Krauss, J. Im, J. A. Schultz, *Annu. Rev. Mater. Sci.* **1998**, *28*, 375.
[35] T. Tani, Z. K. Xu, D. A. Payne, in *Ferroelectric Thin Films III*, Vol. *310* (Eds: E. R. Myers, B. A. Tuttle, S. B. Desu, P. K. Larsen), Materials Research Society, Pittsburgh **1992**, p. 269.
[36] Y. Bastani, N. Bassiri-Gharb, *Acta Mater.* **2012**, *60*, 1346.
[37] R. A. Assink, R. W. Schwartz, *Chem. Mater.* **1993**, *5*, 511.
[38] R. W. Schwartz, P. G. Clem, J. A. Voigt, E. R. Byhoff, M. Van Stry, T. J. Headley, N. A. Missert, *J. Am. Ceram. Soc.* **1999**, *82*, 2359.